Carbohydrate Polymers 306 (2023) 120604

Contents lists available at ScienceDirect

Carbohydrate Polymers

journal homepage: www.elsevier.com/locate/carbpol

Pectin-based aerogel particles for drug delivery: Effect of pectin composition on aerogel structure and release properties

D.A. Méndez [a], B. Schroeter [c], A. Martínez-Abad [a,b], M.J. Fabra [a,b], P. Gurikov [d], A. López-Rubio [a,b,*]

[a] Food Safety and Preservation Department, Institute of Agrochemistry and Food Technology (IATA-CSIC), Valencia, Spain
[b] Interdisciplinary Platform for Sustainable Plastics towards a Circular Economy- Spanish National Research Council (SusPlast-CSIC), Madrid, Spain
[c] Institute for Thermal Separation Processes, Hamburg University of Technology, Eißendorfer Straße 38, 21073 Hamburg, Germany
[d] Laboratory for Development and Modelling of Novel Nanoporous Materials, Hamburg University of Technology, Eißendorfer Straße 38, 21073 Hamburg, Germany

ARTICLE INFO

Keywords:
Molecular weight
Vanillin
Release kinetics
Beads
Carriers

ABSTRACT

In this work, nanostructured pectin aerogels were prepared via a sol-gel process and subsequent drying under supercritical conditions. To this end, three commercially available citrus pectins and an in-house produced and enzymatically modified watermelon rind pectin (WRP) were compared. Then, the effect of pectin's structure and composition on the aerogel properties were analysed and its potential application as a delivery system was explored by impregnating them with vanillin. Results showed that the molecular weight, degree of esterification and branching degree of the pectin samples played a main role in the production of hydrogels and subsequent aerogels. The developed aerogel particles showed high specific surface areas (468–584 m^2/g) and low bulk density (0.025–0.10 g/cm^3). The shrinkage effect during aerogel formation was significantly affected by the pectin concentration and structure, while vanillin loading in aerogels and its release profile was also seen to be influenced by the affinity between pectin and vanillin. Furthermore, the results highlight the interest of WRP as a carrier of active compounds which might have potential application in food and biomedical areas, among others.

1. Introduction

The development of delivery systems is an area of immense importance for human health and wellbeing, having applications in the food, pharma and cosmetic industries. In this sense, aerogels from biopolymers are especially attractive due to their stability, availability, renewability and low toxicity (Mehling et al., 2009). The remarkable aerogels properties (homogeneous structure, tuneable mesh size, interconnected pores, and increased surface area) are advantageous features for exploring the capabilities of aerogels as carrier systems (García-González et al., 2021). Moreover, the so-called second generation of aerogels (which have shifted from inorganic to organic-based ones) has facilitated the penetration of these materials in the food market since they consist on biopolymer-based aerogels, including food-grade polysaccharides and proteins (Manzocco et al., 2021). However, the evaluation and feasibility of different biopolymers for aerogel uses are still in early research phases, because a number of factors including biopolymer source, extraction process, seasonality, and gelation process among others, drastically affect the properties and functionality of the obtained aerogel materials. Among the potential biopolymer sources, fruit and vegetable wastes have a huge potential being among the categories of residues with the largest production (Esparza et al., 2020) and rich in many functional biopolymers of interest. As an example, pectin obtained from novel sources open up the possibility to new applications and improvements (Chen et al., 2016), also satisfying the increasing demand for pectin polymer already existing in the food sector.

Different authors have characterized and evaluated the potential of pectin as an aerogel material and drug carrier mainly from commercial citrus pectins (García-González et al., 2012, 2015; Groult et al., 2021a, 2021b; Groult & Budtova, 2018; Ne et al., 2018; Preibisch et al., 2018; Veronovski et al., 2014; White et al., 2010). However, to the best of our knowledge, these studies emphasized in the structural and mechanical properties of the developed aerogel and in the gelation mechanism, not considering the intrinsic factors related to the compositional and chemical characteristics of the pectin itself which, as can be noticed in other pectin applications, played a key role in the thickening, emulsifier and gelation process. It should be highlighted that pectin has been considered a prebiotic fibre as it is resistant to protease and amylase

* Corresponding author at: Food Safety and Preservation Department, Institute of Agrochemistry and Food Technology (IATA-CSIC), Valencia, Spain.
E-mail address: amparo.lopez@iata.csic.es (A. López-Rubio).

https://doi.org/10.1016/j.carbpol.2023.120604
Received 29 September 2022; Received in revised form 9 January 2023; Accepted 16 January 2023
Available online 21 January 2023

enzymes, both of which are active within the upper gastrointestinal tract, thus being used by gut bacteria in the lower gastrointestinal tract. Therefore, it could be a promising drug vehicle from the mouth to the colon (Veronovski et al., 2014). However, factors such as the pectin structure, composition, and physicochemical properties, may affect the aerogel formation and the interaction with the drug of interest.

Watermelon rind, with a very high global production, is a promising source of pectin. Several works have optimized the extraction conditions from watermelon rind pectin (WRP) and, its structure and properties have demonstrated the potential of this novel pectin source for a number of applications (Campbell et al., 2015; Hartati & Subekti, 2015; Mendez et al., 2021; Méndez et al., 2021; Petkowicz et al., 2017; Zubairu et al., 2018). However, the ability of different pectin samples to form gels depend on their sources and extraction process as they are greatly affected by important parameters such as molecular weight distribution, degree of esterification, structure distribution and compositional sugars (Méndez et al., 2021; Veronovski et al., 2014). Based on previous studies, it was evidenced that the degree of esterification of the WRP extracted is usually >50 % (Méndez et al., 2021), which is not favorable for gel formation through crosslinking with divalent cations and further aerogel production. Different enzyme treatments were evaluated for tailoring the rheological properties of WRP (Méndez et al., 2022), and it was observed that the application of pectin methyl esterase (PME) combined with Endo-1,5-α-arabinanase resulted in the best treatment to produce improved gel strength with divalent cation addition.

In light of the above, it was hypothesized that depending on the structural, physicochemical properties and concentration of pectin, the aerogel structure and its suitability as drug delivery systems can be significantly affected. Therefore, the aim of this work was to evaluate an enzymatically modified WRP for aerogel bead production and to compare it with three commercially available citrus pectin samples with different compositions in order to determine how the intrinsic properties of pectin can affect the morphology and physical properties of the aerogels. The evaluation of these pectin-based aerogels as delivery systems was also carried out using vanillin as a model compound. Vanillin was selected as a hydrophilic drug model just to explore how the properties of the different pectin matrices affect its release. It worth mentioning that vanillin (4-hydroxy-3-methoxybenzaldehyde) is a phytochemical generally regarded as a safe (GRAS) flavouring compound widely used in ice creams, beverages, biscuits, chocolate, confectionery, desserts, etc. (Rupasinghe et al., 2006). Moreover, its bioactive properties, including antimicrobial, antioxidant, anticarcinogenic activities (Sinha et al., 2009), medium polarity and the simplicity to track its release via UV–Vis spectroscopy, make it a perfect candidate as a model active compound to test the release kinetics from porous polymer-carriers. Both aerogel formation and vanillin impregnation were done through supercritical CO_2 treatments and a detailed study on the effects of initial pectin composition on the final structural and release properties of the materials was carried out.

2. Materials and methods

2.1. Material

Three commercially available citrus pectins and an in-house produced and enzymatically modified watermelon rind pectin (WRP) were used in this study: a low methoxy (5 %) citrus pectin (denoted as C1 from now on that was supplied by Megazyme Ltd., (Wicklow, Ireland) and two other citrus pectin of low (C2) and high molecular weight (C3) kindly provided by Herbstreith and Fox KG, (Neuenbürg/Württ, Germany). Watermelon rind pectin was produced at laboratory conditions and enzymatically modified with an endo-1,5-α-arabinanase and a methyl-esterase as previously reported (Méndez et al., 2022)Anhydrous ethanol was provided by Carl Roth GmbH & Co. KG (Karlsruhe, Germany).

2.2. Pectin characterization

2.2.1. Carbohydrate composition

The sugar composition of the extracts was determined after acidic methanolysis as previously described (Méndez et al., 2022). Freeze-dried samples (1 mg) were incubated with 1 mL of 2 M HCl in dry methanol for 5 h at 100 °C. Samples were then neutralized with pyridine, dried under a stream of air, and further hydrolysed with 2 M TFA at 100 °C for 1 h. The samples were again dried under a stream of air and re-suspended in milliQ, filtered and injected. The monosaccharides were analysed using high performance anion exchange chromatography with pulsed amperometric detection (HPAEC-PAD) with a ICS-6000 system (Thermofisher) equipped with a CarboPac PA1 column (4 × 250 mm, Dionex). Control samples of known concentrations of mixtures of glucose (Glc), fucose (Fuc), rhamnose (Rha), galactose (Gal), arabinose (Ara), xylose (Xyl), mannose (Man), galacturonic acid (GalA) and glucuronic acid (GlcA) were used for calibration (Merck, Germany).

2.2.2. Ash content

The ash content was determined according to the standard method TAPPI T211 om-07. All measurements were carried out in triplicate.

2.2.3. Protein content

The protein content was carried out by the Dumas combustion method (nitrogen conversion factor 6.25) according to ISO/TS, 16634–2 (2016).

2.3. Molecular weight distribution

The molecular weight of the pectin was estimated by HPSEC using Waters ACQ Arc Sys Core 1–30 cm CH (Waters, USA). The HPLC system was equipped with a Waters 2998 PAD module, a Waters 2414 refractive index detector (Waters, USA), and 2475 FLR module (Waters, USA). 0.1 M NaCl was used as the mobile phase. The samples (3 mg/mL) were dissolved in the mobile phase under magnetic stirring at 40 °C, filtered through 0.22 μm pore syringe filters. Then, the samples were injected into columns in series (PolySep-GFC-P 4000 and 2000 (300 mm × 7.8 mm) Phenomenex Inc., CA, USA) equilibrated at 40 °C. The injection volume was 20 μL and the flow rate was 0.5 mL/min. Calibration was performed using a pullulan standards kit (PSS polymer standards service GmbH, Mainz, Germany).

2.4. Rheological characterization

The viscosity of the pectin solutions was determined using a rheometer HR20, (TA Instruments, Montreal, QC, Canada) with a 40 mm parallel plate geometry. Briefly, pectin solutions at 2 % (w/w) and 4 % (w/w) were dissolved in deionized water and adjusted to pH 4.0. Samples were loaded on the bottom Peltier plate. The viscosity was measured by rotational shear between the two parallel plates at 20 °C with a gap of 500 μm as a function of increasing shear rate from 0.1 s^{-1} to 200 s^{-1}. The samples were recorded with the TRIOS software version 5.1.1.46572 (TA Instruments, Montreal, QC, Canada. The power law model Eq. (1) was applied to determine the consistency index (k) and the flow index behaviour (n). The apparent viscosities were determined at 100 s^{-1}.

$$\sigma = K\gamma^{n} \quad (1)$$

2.5. Preparation of hydrogel beads and particles

2.5.1. Dripping method

Pectin solutions at 2 and 4 % (w/w) in de-mineralized water were prepared and pH adjusted to 4.0 to avoid acidic induced gelation during the process (Groult & Budtova, 2018). The solutions were extruded at 4 mL/min through a stainless-steel needle (0.4 mm inner diameter) into an

aqueous gelation bath containing $CaCl_2$ at 0.5 % (w/w) which was slowly agitated with a magnetic stirrer. The distance between the syringe tip and the coagulation bath was 3 cm. After bead formation, the beads were kept in the coagulation bath for 24 h to stabilize the gel network.

2.5.2. Jet cutting method

Hydrogel particles were produced with the JetCutter Type S from geniaLab GmbH, Braunschweig, Germany. A gelation bath was previously prepared at 0.5 % (w/w) of $CaCl_2$ as a crosslinker. Four process parameters were fixed: the cutting frequency (f_{cut} 2000 rpm), the nozzle diameter (d_{nozzle} = 0.3 mm), the jet flow (F_{jet} = 0.25 g/s), the falling distance (1.5 m) and the pectin solution concentrations of 2 and 4 % (w/w).

2.6. Aerogel production

A sequential solvent exchange was carried out by immersion of the resulting hydrogels in 20, 40, 60 and 80 wt% ethanol for 24 h each. Then, the samples were immersed in 99.9 wt% ethanol until a minimum final concentration of 98 wt% ethanol inside the hydrogels was reached (controlled by density measurements, Anton Paar, DMA 4500 M). A hydrogel solvent ratio of 1:10 was kept during the solvent exchange.

After the solvent exchange, the alcogel particles and beads were sealed into a filter paper bag and placed into a high-pressure autoclave with an overall volume of 3.9 L for supercritical drying with CO_2. The supercritical drying was performed at a temperature of 60 °C and pressure of 120 bars. A continuous flow of CO_2 (flow rate = 80–110 g/min) was set through the autoclave until complete extraction of the ethanol was achieved after 4 h. The aerogel materials were collected after slow de-pressurization (1 bar/min) of the autoclave and stored in sealed tubes (25 mL, Sarstedt) in a desiccator prior to analysis.

2.7. Supercritical impregnation with vanillin

Vanillin was selected due its proven good solubility under supercritical conditions (temperature 34.8–44.8 °C, pressure 85–500 bars) (Liu et al., 2006; Rojas-Ávila et al., 2016), and proven impregnation efficiency on aerogels, as previously reported by Schroeter, Yonkova, Goslinska, et al. (2021). For the impregnation process, vanillin was placed at the bottom of the high-pressure autoclave keeping an aerogel: vanillin weight ratio of 1:2 (g/g). The aerogel materials were sealed into a filter paper bag. The supercritical impregnation was performed in a closed system at a temperature of 60 °C and pressure of 120 bars of supercritical CO_2 for 16 h. The impregnated material was collected after slow depressurization (1 bar/min) of the autoclave and stored in sealed tubes (25 mL, Sarstedt) in a desiccator prior to analysis. The drug loading capacity (LC) was determined according to Eq. (2).

$$LC(\%) = \frac{\text{Total mass of the loaded aerogels} - \text{Mass of dried aerogels}}{\text{Total mass of the loaded aerogels}} * 100\% \quad (2)$$

2.8. Aerogel characterization

The bulk density of aerogel particles and beads were measured using a graduated cylinder. Dry and impregnated aerogel particles (0.3 g) were filled in the cylinder up to a certain volume without tapping. The bulk density was calculated as a ratio of the weight and the occupied volume.

Furthermore, low temperature N_2 adsorption–desorption analysis was performed to investigate microstructural properties of the aerogels (Nova 3000e Surface Area Analyzer, Quantachrome Instruments, Boynton Beach, USA). A single determination was carried out for aerogel produced. An overall sample mass of 20–30 mg was used for each analysis. The specific surface area was determined using the BET (Brunauer–Emmett–Teller) method (Brunauer et al., 1938). The pore volume (Vpore) and average pore diameter (Dpore) were estimated by the BJH (Barrett–Joyner–Halendia) method (Barrett et al., 1951). All samples were degassed under vacuum at 60 °C for 6 h prior to analysis.

2.9. Scanning electron microscope

The surface properties and the inner structure of the aerogels were characterized via scanning electron microscopy (SEM, Zeiss Supra VP55, Jena, Germany). The intact and cut beads were sputtered with a thin layer of gold (approx. 6 nm thickness, Sputter Coater SCD 050, BAL-TEC) before analysis. The measurements were carried out under high vacuum at an accelerating voltage of 3 kV and a working distance of 4.2–5.6 mm.

2.10. Image analysis

The size and shape of beads via dripping method was determined based on image analysis of pictures. 50 beads per experiment were evaluated to determine the mean particle diameter (Dparticle), perimeter and projection surface area (ImageJ software). In case of irregular shaped beads, the average of the maximum and minimum diameter was used to calculate the Dparticle.

Size and shape of dry aerogel particles from jet cutting process were determined with a Camsizer XT system (Retsch Technology) in free fall mode. All characterizations were carried out according to DIN 66,141. $d_{particle}$ was calculated from the longest feret-diameter and the shortest chord-diameter of each particle projection as follows (Eq. (3)):

$$d_{particle} = \sqrt{x_{Femax}^2 - x_{cmin}^2} \quad (3)$$

where x_{Femax} is the longest feret-diameter and x_{cmin} being the shortest chord-diameter of each particle projection.

2.11. FTIR

FTIR measurements were recorded in transmission mode in a controlled chamber at 21 °C and dry air in order to avoid humidity and CO_2 using a Cary 630 FTIR spectrometer (Agilent, USA). The spectra were taken at 4 cm^{-1} resolution in a wavelength range of 400–4000 cm^{-1} and averaging a minimum of 32 scans. Spectra acquired were processed using Origin pro 2019 software (OriginLab Corporation, Northampton, MA, USA).

2.12. Vanillin release kinetics

A kinetic study on vanillin release from the impregnated aerogel beads prepared at two different pectin concentrations (2 and 4 % (w/w)) in water was monitored using a spectrophotometer (Evolution™ 300, Thermo Fisher Scientific, USA) at 280 nm. Around 180 mg of impregnated bead samples were immersed in 500 mL of distilled water at 30, 40 and 50 °C with magnetic stirring (180 rpm). The range of temperature was selected to evaluate any influence of this factor on vanillin release, also keeping in mind the body temperature which falls within the selected range. At pre-determined time periods, an aliquot (1 mL) from the solution was taken out and analysed, and then returned back into the release medium. The vanillin concentration was calculated through a calibration curve constructed beforehand using vanillin solutions with known concentrations. The kinetic experimental data collected was analysed and adjusted according to previous work (Schroeter, Yonkova, Goslinska, et al., 2021) with the Weibull model approach (Eq. (4)) using origin 9.6 (OriginLab Corporation, Northampton, MA, USA).

$$c_t = c_{max} - e^{-\left(\frac{t}{a}\right)^{\beta}} \quad (4)$$

with c_t being the concentration at time t, c_{max} being the vanillin concentration in the water phase at the end of the measurement. α is the scale constant and β is the shape constant.

2.13. Statistical analysis

All statistical analysis was performed using the statistical software Statgraphics Centurion XVI® (Manugistics Inc.; Rockville, MD, USA). Statistically significant differences were determined by using one-way analyses of variance (ANOVA) and sample comparison with LSD at 95 % confidence level (p-value <0.05).

3. Results and discussion

3.1. Initial pectin characterization

A compositional characterization of the different pectin samples used for aerogel production was conducted in order to assess and correlate composition with their gelling capacity, aerogel structure, subsequent vanillin impregnation and release profiles. The three commercial pectin samples (C1, C2 and C3) showed a high purity, with a total carbohydrate content near to 100 % and very high Gal A content, typical for industrial pectin (Table 1). Only small differences between these citrus pectin samples were found, with a higher content in protein in the low molecular weight citrus pectin (C2) and a slightly higher branching degree in the medium molecular weight pectin (C3). In contrast, the enzymatically-modified watermelon rind pectin (WRP) obtained in the laboratory showed remarkable differences compared to the citrus pectin samples. Specifically, it was a relatively less pure pectin extract due to the presence of a certain amount of protein and ashes and, more interestingly, this WRP had a much larger branching degree pointing out at the predominance of long galactan side chains (Méndez et al., 2021).

The presence of longer branches in the WRP pectin has been seen to affect the rheological properties of the gels formed with Ca^{2+} (Méndez et al., 2022). However, there are other factors which could affect the structure and physical properties of the gels and of the subsequent aerogels, such as degree of blockiness or esterification degree (DE), among others (Ngouémazong, Kabuye, et al., 2012). As observed from Table 1, WRP had the lowest DE and the greatest protein content and branching degree (RB), with a considerable lower homogalacturonan percentage, thus suggesting less gel strength as observed in previous works with WRP compared with C1 (Méndez et al., 2022; Ngouémazong, Jolie, et al., 2012) that could be highly co-related to the methyl-esterification pattern and available junction zones (Ngouémazong, Jolie, et al., 2012).

The FTIR of the various pectin powders showed the typical fingerprint for pectin (Fig. 1A), identified by the two strong absorption bands at 1012 and 1084 cm^{-1} which are attributed to glycosidic linkages (C—O and C—C stretching bonds) and is typical for backbone vibrations of pectin (Bichara et al., 2016; Kacuráková et al., 2000; Mikshina et al., 2017; Pasandide et al., 2017). The band at 1077 cm^{-1} has been previously attributed to neutral Ara-based glycans or RG regions (Kacuráková et al., 2000). Other characteristic pectin FTIR vibrational bands are the one at 1730 cm^{-1}, ascribed to esterified carbonyl groups (C═O), the band at 1598 cm^{-1}, corresponding to free carboxylic groups COO^-, and another symmetric vibrational band at 1406 cm^{-1} which is also related to the free carboxyl groups (Kozioł et al., 2022; Pasandide et al., 2017). Due to the low degree of esterification in all selected pectins (low methoxy degree), a high intensity is observed for the bands representative for free carboxylic (1598 cm^{-1}) groups (Gnanasambandam & Proctor, 2000; Méndez et al., 2021) which is desirable for divalent cation interaction and hydrogel-forming.

Another factor which is closely related to the rheological behaviour of pectin is the molar mass distribution (MM) (Fig. 1B), as apart from affecting the viscosity of pectin solutions, also plays a key role in the gelation process itself and in the shape of the gels and final aerogel structure (Schroeter, Yonkova, Niemeyer, et al., 2021). A broad polydisperse peak was observed for the three industrial pectin samples (C1, C2 and C3). In contrast, a much narrower MM was observed for the WRP pectin, which could be a result of the specificity of the enzymatic process and subsequent dialysis steps. WRP had a very similar average MM as the C2 sample (the lower molecular weight pectin) and C3 sample showed the broadest distribution. Smaller peaks (lower than 1.5 kDa) were observed for samples C1, C2 and C3, that were higher with the increase arabinose content of each sample, which is in accordance with previous reports (Brigand et al., 1990). Interestingly, the WRP also showed three less intense peaks under 2.3 kDa that probably corresponds to the degradation products of pectin or the associated lignin (Sun & Hughes, 1998). These differences may be due to the different extraction conditions, pectin source and the harvest conditions (el Fihry et al., 2022).

The rheological behaviour of pectin solutions was also evaluated as it has been considered a key factor in the production of quality hydrogel beads. Higher viscosities usually induce more spherical beads resistant to impact forces when hitting the coagulation bath surface (Schroeter, Yonkova, Niemeyer, et al., 2021). As expected, higher pectin concentrations (e.g. 4 % (w/w)) resulted in increased viscosity and a more shear thickening behaviour ($n < 1$) (see Table 2). At the lower pectin concentration (2 % (w/w)), the apparent viscosity of the solutions was related with their MM, being the C3 pectin the one giving raise to the more viscous solutions, followed by C1. In the case of C2 and WRP, as shown in Fig. 1C, at 2 % (w/w) concentration, C2 showed a higher apparent viscosity than WRP only at lower shear rates. At higher shear rates, the hydrophobic interaction caused by the higher DE which is related to more viscous pectins, was surpassed and their resistance to shear stress was lowered as expected for the reduced MM (Chan et al., 2017). Furthermore, it was observed a high standard deviation during the first shear rate steps, due to the low viscosity and high variability during the polymer reorganization of this sample. At higher pectin

Table 1
Composition of pectin samples. Degree of esterification (DE %), protein and ash content (%) and structural ratio of pectin powder C1, C2, C3 and WRP.

Sample	DE %****	Ashes (% d.w.)	Protein content (%)	Rha (μg/mg)	Ara (μg/mg)	Gal (μg/mg)	GalA (μg/mg)	RB*	RL**	HG %***
C1	5	0.47(0.01)^a	5.78(0.07)^c	45.1(6.41)^a	7.02(0.98)^a	91.28(15.54)^a	856.42(132.05)^a	2.2	5.8	81.1
C2	6.5	3.08(0.08)^b	7.44(0.004)^b	43.32(0.66)^a	17.05(0.34)^b	91.36(6.66)^a	885.94(43.87)^a	2.5	5.6	84.2
C3	5.6	1.91(0.00)^c	5.82(0.08)^c	41.05(4.81)^a	23.72(3.01)^c	98.9(10.87)^a	831.97(89.53)^a	2.9	4.9	79.1
WRP	4.8	1.47(0.02)^d	7.95(0.021)^a	19.4(3.52)^b	1.72(0.13)^d	120.14(3.58)^b	633.35(46.05)^b	6.2	4.4	61.4

Numbers in brackets corresponds to standard deviation.
The rest of sugars were detected in minor amounts (See supplementary material Fig. S1).
The data are averages and standard deviations (brackets) of triplicate measurements. Values in each column with different superscript letters (a-d) indicates significant differences ($p < 0.05$) among samples.
* RB A larger value is indicative of larger average size of the branching side chains. (Gal+Ara/Rha).
** RL A larger value suggest of more linear/less branched pectins. (GalA/(Xyl + Rha + Ara + Gal).
*** (GalA-Rha).
**** DE values were given by the suppliers, DE of WRP was estimated according to the method described in Méndez et al. (2022).

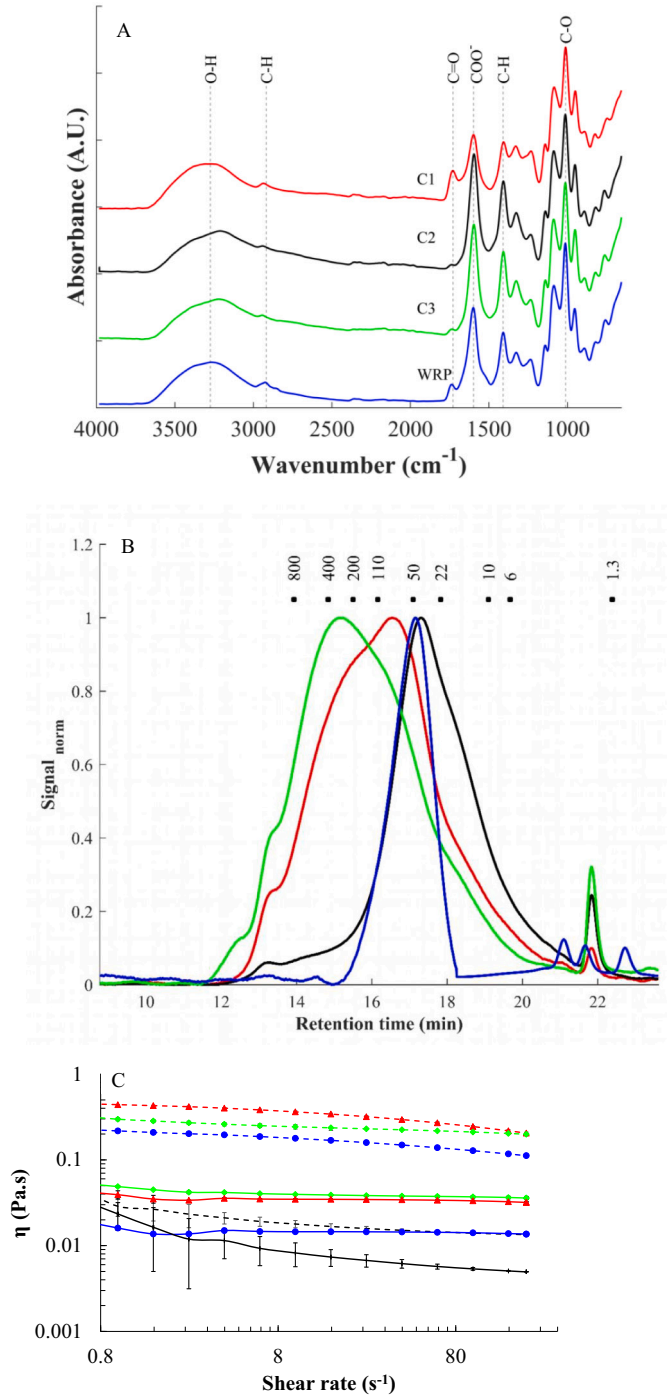

Fig. 1. (A) FT-IR spectra for initial pectin powder C1, C2, C3 and WRP. (B) Molar mass (MM) distribution of the pectin samples, the black squares correspond to pullulan standards with the matching MM. (C) Apparent viscosity vs. shear rate curves for solutions prepared with, at 2 % (w/w) (continuous line) and 4 % (w/w) (dotted line) pectin concentration, WRP (■), C1 (■), C2 (■), and C3 (■).

concentration, the closer polymer-polymer interactions affected the rheological behaviour and, although the MM distribution was displaced towards lower molecular weights for the C1 pectin, a greater resistance to shear stress was observed probably ascribed to better electrostatic interactions among the pectin chains (Chan et al., 2017; Petkowicz et al., 2017). On the other hand, although samples WRP and C2 share similar MM, WRP had a superior viscosity. This suggests that the branching degree (RB) had a significant impact in the viscosity and rheological properties, caused by the entanglements interactions as previously reported for branched pectin gels (Ngouémazong, Kabuye, et al., 2012; Petkowicz et al., 2017).

Table 2
Flow behaviour index (n), consistency index (k) and apparent viscosity (η_{ap}) of the pectin solutions prepared at (A) 2 and (B) 4 % (w/w).

Sample	n	K	R^2	η_{ap} (Pa.s) at 100 s^{-1}
C1 (A)	0.97	0.03	0.999	0.033
C1 (B)	0.85	0.4	0.998	0.244
C2 (A)	0.77	0.015	0.997	0.005
C2 (B)	0.85	0.026	0.998	0.014
C3 (A)	0.96	0.04	0.999	0.037
C3 (B)	0.93	0.28	0.999	0.210
WRP (A)	0.98	0.014	0.999	0.014
WRP (B)	0.87	0.22	0.999	0.129

3.2. Development and characterization of aerogels beads

The substantial differences found among the pectin samples studied were expected to affect the microstructure and release properties of aerogel beads produced thereof. Initially, the effect of pectin concentration on aerogel structure was evaluated. To this end, pectin hydrogels were initially obtained by dripping pectin solutions (at 2 % and 4 % (w/w)) onto a gelling bath containing 0.5 % (w/w) $CaCl_2$ and subsequently, aerogels from the four different pectin samples were obtained through supercritical drying. The average diameter for hydrogel beads was 2.89 ± 0.2, 3.43 ± 0.3, 2.8 ± 0.1 and 2.48 ± 0.2 mm for C3, C2, C1 and WRP samples respectively (Table S1. supplementary material), at 2 % (w/w). At higher pectin concentrations, the size of the beads increased around 20 % for samples C2, C3 and WRP. Interestingly, the size of the aerogel particles prepared with C1 increased- 66 % at 4 % (w/w), which was presumably ascribed to the higher viscosity, increasing the size of the drop during the dripping process.

Fig. 2 shows representative images of the visual appearance of the various pectin gels before (hydrogels and alcogels) and after (aerogels) supercritical drying. As observed from this Figure, the morphology of the hydrogel, alcogel and aerogel structures depended on the pectin source. Round shape hydrogel and alcogel capsules obtained from WRP presented a whitish hue which could be ascribed to the presence of some impurities (like proteins) with different refractive indices which provoked light dispersion. In contrast, those prepared with commercial citrus pectin were more transparent, indicative of a greater homogeneity. Besides, it is worth mentioning that C1 and C3 pectin gave rise to round shaped and translucent beads whereas capsules prepared with C2 had a noticeable irregular shape after the gelling process, even in those prepared at the higher pectin concentration. This suggests that not only the esterification degree but also the molecular weight, linearity and purity played a role on the gel's formation. The significantly lower viscosity of C2 together with the greater DE and protein content could explain the morphology obtained in this case, in agreement with previous research studies (Fitri et al., 2021; Schroeter, Yonkova, Niemeyer, et al., 2021; Shi et al., 2011).

In order to quantitatively evaluate the morphological changes related to the type of pectin used, the sample volumetric shrinkage was monitored from hydrogel to aerogel for samples prepared at 2 and 4 % (w/w) pectin and the results are displayed in Fig. 3. The shrinkage phenomenon has been frequently reported for other pectin and bio-based aerogels, and it is an important parameter for evaluating the quality of aerogels in terms of preservation of the fragile microporous structure, dimensional stability and quality of the aerogel pore system (Chartier et al., 2022; Dirauf et al., 2021; El-naggar et al., 2020; Groult et al., 2021a; Liebner et al., 2009; Schroeter, Yonkova, Niemeyer, et al., 2021). A multistep solvent exchange was used as it has been reported to greatly limit the shrinkage phenomenon. However, at lower pectin concentrations, a significant size reduction was observed already during

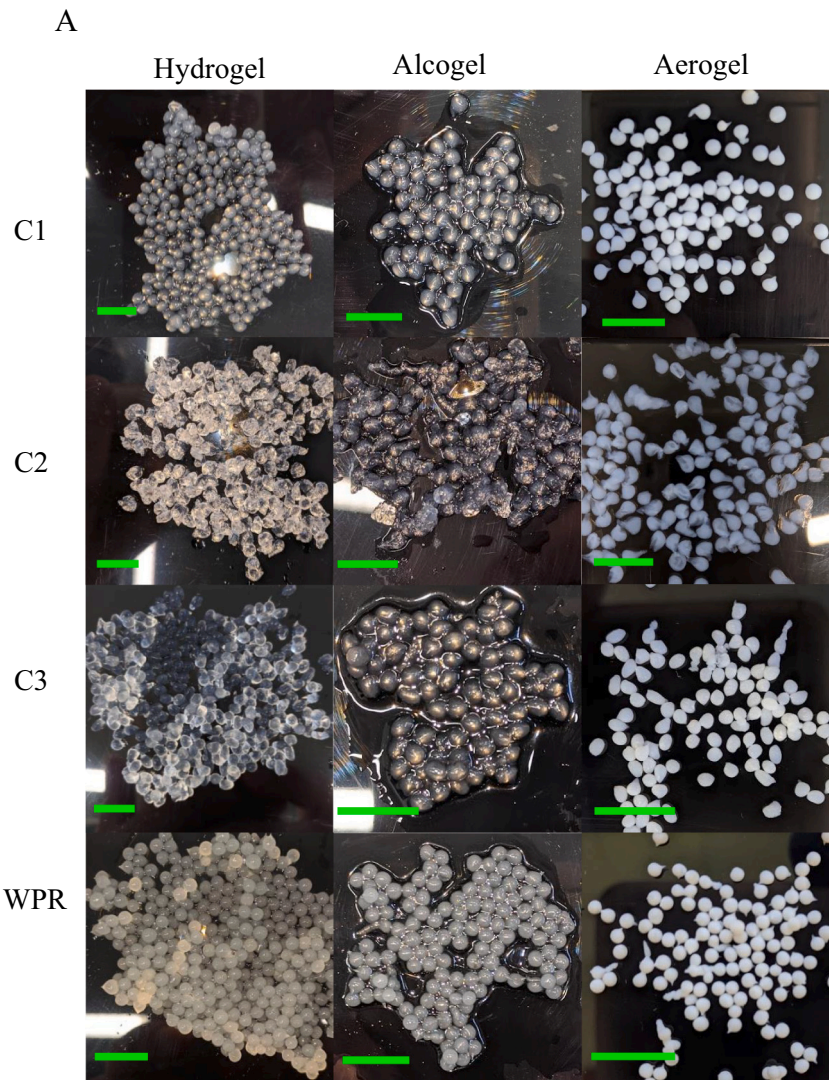

Fig. 2. Beads produced by dripping method with gelation bath at 0.5 % (w/w) $CaCl_2$ at two pectin concentration solution a) 2 % (w/w) and b) 4 % (w/w). (green scale bar corresponds to 1 cm).

solvent exchange process. This phenomenon has been previously reported, as hydrogels with low solid contents are prone to significant shrinkage, losing about half of their volume during solvent exchange (Gurikov et al., 2019). In contrast, shrinkage decreased with the increase of pectin concentration, as previously reported for other aerogels, as more concentrated solutions are generally more robust, undergoing less changes during solvent exchange and subsequent drying (Groult & Budtova, 2018; Gurikov et al., 2019). From Fig. 3, one could see the relevance of the homogalacturonan (HG) content and DE in the shrinking phenomenon and, thus, the commercial C3 pectin, with a 79 % HG content and DE 5.6 exhibited the greatest shrinkage, even when prepared at the higher concentration (4 % (w/w)). While the WRP had a substantially lower HG content of 61 %, the lower DE (4.8 %) partially prevented shrinkage during aerogel formation, probably due to a stronger hydrogel network formed through the interactions between free carboxyl groups and the positively charged divalent ions present in the gelation bath. The C1 pectin, having the lowest DE (5) and a high HG content (81 %), probably leading to the strongest hydrogels, was the one suffering from less shrinkage, especially at the higher pectin concentration. Other factors which affect gel strength are also expected to influence the shrinkage degree. Interestingly, a substantial shrinkage was observed in C3 pectin at the greater concentration (cf. Fig. 3b), which seems to point out the greater degree of branching, responsible of its greater molecular weight and probably leading to a lower gel strength. In fact, similar effects were previously reported for polyethylene aerogels (Khedaioui et al., 2019; Leven et al., 2021; Liebner et al., 2009). Rodríguez-Dorado et al. (2019) also reported that high molecular weight alginate induced a higher shrinkage degree and less porous materials.

Therefore, it could be concluded that the shrinkage phenomenon was not only affected by the biopolymer concentration, as it has been previously reported, but also by compositional, structural, molecular interactions and the collapse due to surface tension effects at the vapor–liquid interfaces (Benali & Boumghar, 2014; Groult & Budtova, 2018; Schroeter, Yonkova, Niemeyer, et al., 2021).

The microstructure and porosity of the aerogels formed were also examined by scanning electron microscopy (SEM). Fig. 4 shows representative micrographs of the inner structure of the aerogel capsules formed using WRP and the commercial pectin samples (C1, C2 and C3) prepared at both concentrations. Although a porous three-dimensional network was observed in the different samples, from the SEM images it was difficult to draw conclusions about the microstructure and, thus, the surface area, bulk density and average pore size were measured through the BET method and the results are displayed in Table 3.

Table 3 displays the surface area, bulk density, and average pore

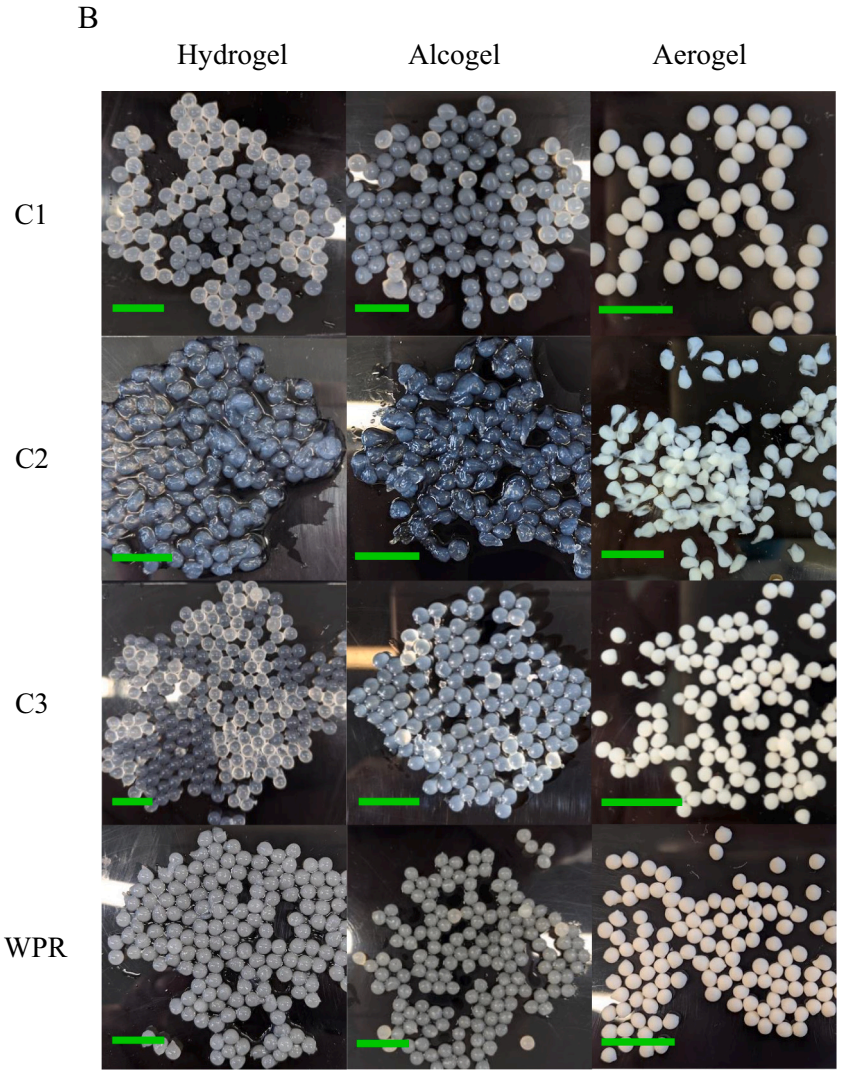

Fig. 2. (*continued*).

diameter of the various pectin aerogels. In general, the specific surface area of the aerogels ranged between 469 and 585 m^2/g, in agreement with previous works (Preibisch et al., 2018; Veronovski et al., 2014). Interestingly, while surface area could not be directly related with shrinkage, the bulk density clearly reflected the changes taking place during aerogel formation. In fact, while the surface area of the developed aerogels did not significantly increase as the pectin concentration increased, as it was the case in previous studies (Buchtová & Budtova, 2016; Chartier et al., 2022; Groult & Budtova, 2018), concentration and shrinkage affected the bulk density of the samples, being the C1 and C2 the samples with lower values, in accordance with their lower shrinkage observed. These lower bulk densities were also correlated with greater average pore diameters (cf. Table 3). pore volume varying from 2.37 to 8.65 cm^3/g, with noticeable changes among samples (Supplementary material, Table S4). The fact that increasing the pectin concentration did not lead to a significant increase in the surface area, could be related to the $CaCl_2$ concentration used as a crosslinker, which was fixed at 0.5 % (w/w) and, therefore, the amount of calcium ions able to interact with ionized groups of non-methylated galacturonic acid on the pectin backbone was limited (Dronnet et al., 1996; Groult & Budtova, 2018; Thibault & Rinaudo, 1986). Bulk density values were in agreement with the results recently reported by (Groult et al., 2021b), C3 and WRP aerogels presented greater bulk densities, explained by their greater shrinkage degree.

The various aerogels formed were up-scaled through a jet cutting methodology to check on the validity of the conditions used and the results are shown in the supplementary material (cf. Table S3 in the Supplementary Material) which confirmed the reproducibility of the methodology used.

3.3. Pectin aerogels as drug delivery systems

In the last part of this work, highly porous pectin aerogels obtained by means of the dripping methodology were subsequently impregnated with vanillin and the drug loading efficiency and kinetics release were analysed. The impregnation process provided a brief insight of possible chemical interaction and affinity between pectin and vanillin. During the impregnation process, the aerogel beads suffer a size reduction of 8.4, 9.0, 3.1 and 15 % for C1, C2, C3 and WRP respectively, as the structure collapses due to the high pressures in the supercritical impregnation process (Fig. S2. Table S1 Supplementary material). As observed in Table 3, the loading capacity efficiency varied between 9 % and 60 %, in agreement with previous works using other biopolymers (García-González et al., 2015; Groult et al., 2021b; Mehling et al., 2009; Tkalec et al., 2016; Veronovski et al., 2014). It is worth mentioning that the loading capacity was significantly higher and very similar in all the pectin aerogels prepared at 2 % (w/w) concentration. In contrast, lower vanillin loading was observed when increasing pectin concentration.

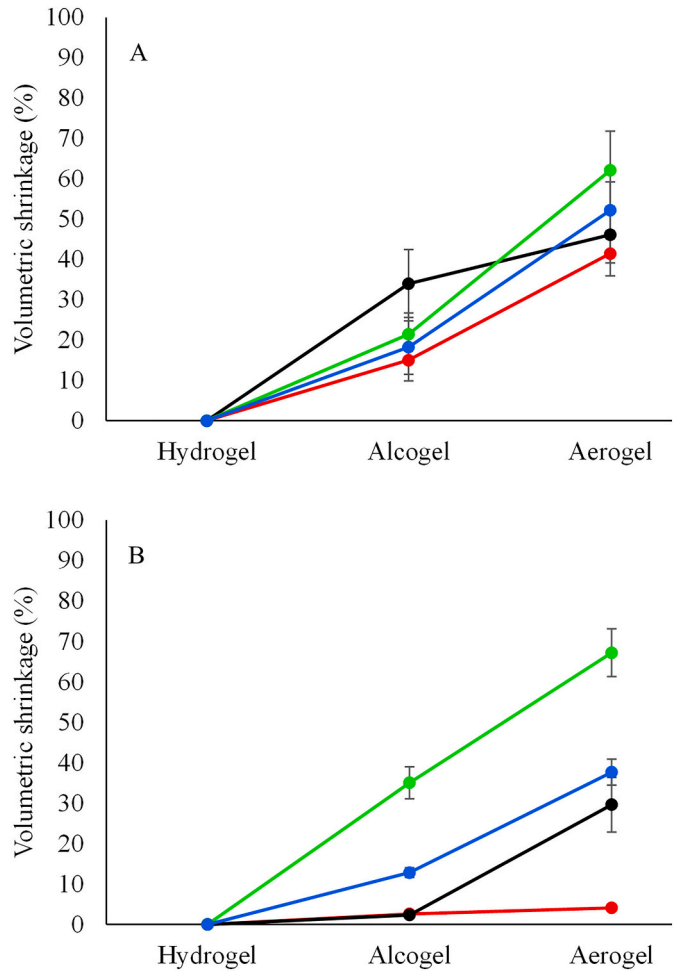

Fig. 3. Volumetric shrinkage during the aerogel preparation (C1 (■), C2 (■), C3 (■) and WRP (■)) as a function of pectin concentration: A) 2 % (w/w) and B) 4 % (w/w). The hydrogels were formed by dripping the pectin solutions in a 0.5 % (w/w) $CaCl_2$ coagulating bath. Lines are drawn to guide the eye.

The results seem to point out to the low chemical affinity between vanillin and low methoxy pectin. Vanillin is a phenolic aldehyde with three functional groups (aldehyde, ether and hydroxyl groups), with a tendency to form aggregates stemming from the hydrophobicity of aromatic compounds (Frenkel & Havna-Frenkel, 2006). The results seem to indicate that at low pectin concentrations, most of the carboxyl groups from pectin are interacting with the calcium cations to form the so-called egg-box junctions, leaving a relatively hydrophobic inner aerogel structure, where vanillin molecules can penetrate and stack together and, thus, similar loadings were observed irrespective of the pectin used. In contrast, at high pectin concentrations, only some of the carboxyl groups were interacting with the calcium ions, thus leaving a more hydrophilic environment within the aerogels. In this case, the composition of the various pectin samples affected aroma loading. C1 pectin, having the lower DE, a high homogalacturonan content, the lower protein content and a low shrinkage, was the one having less vanillin affinity and thus, displaying the lower loading capacity. C2 and C3 pectin aerogels displayed the greatest vanillin loading when prepared at 4 % (w/w) pectin concentration, probably ascribed to their higher DE, thus presenting a more hydrophobic inner aerogel environment. Interestingly, WRP, even though having the lowest DE, was able to incorporate much more vanillin than the C1 aerogels, explained by the lower HG content (61 %) and greater protein content, as aromatic compounds such as vanillin are prone to interact with proteins (Tromelin et al., 2006).

3.4. Release kinetics

The release kinetics are influenced by the drug and carrier material. For instance, when a hydrophilic drug is loaded into a hydrophilic aerogel, hydration and drug dissolution are often fast, facilitating drug desorption. Likewise, different phases could occur depending on the interaction with the media, such as erosion, swelling, and in some cases, dissolution of the carrier matrix. During the first phase, hydration and swelling of the carbohydrate-based aerogels normally takes place, finally resulting in the collapse of the pores and the formation of a hydrogel-like matrix. It has been reported that the velocity of the pore collapse and hydrogel formation affects drug release kinetics (García-González et al., 2021), which will be affected by the pectin type, pectin-vanillin interactions and release media.

Based on drug load capacity (LC) results, a complete release was detected in all cases, at the end of the measurement. Furthermore, the total loaded vanillin of the aerogel beads was verified with prolonged times where no changes in concentration in the release media were noticed. In order to characterize the vanillin release profiles from the various pectin aerogels, a Weibull model-based approach was used for description of release kinetics. While the approach is purely empiric, it has demonstrated suitability for highly correlated non-linear kinetic description of chemical reactions in previous works (Kokkinidou et al., 2014; Schroeter et al., 2019; Schroeter, Yonkova, Goslinska, et al., 2021). In this work, the influence of temperature was also evaluated (30, 40 and 50 °C) but according to the kinetic data, vanillin release was temperature-independent (see Fig. S3 in the Supplementary Material), supporting the hypothesis of low pectin-vanillin interactions, indicating, that vanillin was not covalently attached to the aerogels, and thus, the diffusion driven process, was only slightly dependent on temperature. Therefore, the rate constants were calculated from the average profiles of the three kinetic release temperatures. Vanillin release profiles of all samples were fitted with a high correlation (R^2 0.985–0.999) up to complete release by the Weibull model, except the C3 aerogel at 2 % (w/w), which showed a differentiated release behaviour starting with a linear release (0 order) followed by a swelling step up to ~ 80 % and a final slower release (Fig. 5). The data from Table 4 indicate that release kinetics, at least during the first minutes, were mainly influenced by aerogel shrinkage, bulk density and average pore size and, thus, the greatest shrinkage experienced by the C3 aerogel obtained with a pectin concentration of 4 % (w/w), probably hindered water diffusion within the aerogel, thus limiting the initial vanillin release. WRP also showed slower initial vanillin release, also explained by the lower average pore size limiting solvent diffusion. However, in the case of WRP, once the water penetrated within the structure, a burst vanillin release occurred, again confirming the low chemical affinity between both materials.

The obtained data showed a faster release kinetics compared with previous works from cellulose aerogels loaded with vanillin (Schroeter, Yonkova, Goslinska, et al., 2021) and pectin aerogels loaded with theophylline (Groult et al., 2021a). The use of aerogels for fast release is also desirable in some cases, e.g. in drug release for dermal treatments (Siepmann & Siepmann, 2012).

4. Conclusions

Three commercial citrus pectin samples (C1, C2 and C3) and an enzymatically-modified watermelon rind pectin (WRP) with different physicochemical characteristics were investigated for the production of aerogel beads at two pectin concentrations (2 and 4 % (w/w)) and they were evaluated as potential drug carriers. Results showed that pectin concentration, the degree of esterification, composition and molecular weight, affected hydrogel and subsequent aerogel particle formation. The aerogel particles obtained presented high surface areas and low-bulk density values, thus making them attractive vehicles for delivery

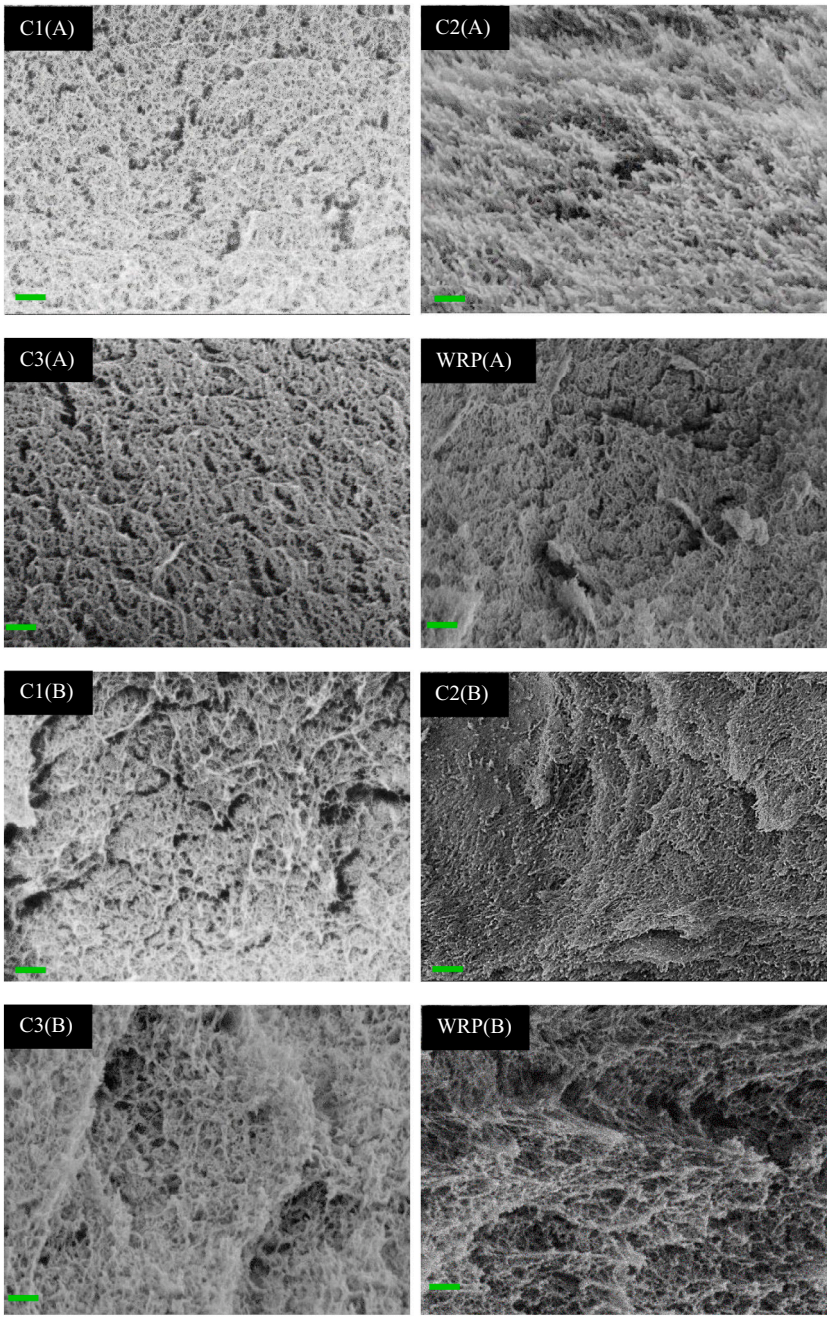

Fig. 4. SEM micrographs of pectin aerogels produced via dripping method at two different concentrations: 2 % (w/w) (A) and 4 % (w/w) (B). Scale markers corresponds to 400 nm.

applications. Shrinkage during aerogel formation was highly dependent on the pectin concentration and structure and, thus, C1 pectin at 4 % concentration, having the lowest DE and a high HG content, was the one with the lowest shrinkage, while C3 and WRP with lower HG contents suffered from substantial shrinkage, thus having higher bulk density values and lower average pore diameters. Vanillin, as a model compound, was loaded by impregnation, in the different aerogel structures. The low chemical affinity between pectin and vanillin explained greater aroma loading in the aerogels prepared at 2 % (w/w) pectin concentration, while the vanillin content of the aerogels prepared with 4 % pectin was seen to depend on the inherent pectin characteristics and, thus, those having more hydrophobic groups were the ones incorporating more vanillin. The low chemical affinity between pectin and vanillin also affected the release kinetics (not influenced by temperature) and, in this case, slower release, especially in the initial phase was observed for the samples with smaller average pore sizes (C3 and WRP), probably due to the limited solvent diffusion towards the inner part of the aerogels. While WRP aerogels could be considered promising carriers of active compounds of interest in the food and pharma areas due to the biocompatibility and potential benefits as a prebiotic compound, limitations due to the fast drug release need to be tackled. Several previous studies reported the use of vanillin as a model active ingredient (Liu et al., 2023; Stanzione et al., 2017), with some strategies for release control, such as coating the aerogel beads (Schroeter, Yonkova, Goslinska, et al., 2021). Further experiments are needed to explore their potential as a carrier of hydrophobic compounds and to mimic human conditions.

Table 3
Surface area (m^2/g), bulk density (g/cm^3), and Dpore (Å), of aerogel samples (C1, C2, C3 and WRP) produced by the dripping method at (A) 2 % (w/w) and (B) 4 % (w/w) of pectin solutions, drug loading capacity LC % (w/w) and bulk density (g/cm^3) of loaded aerogels.

Sample	Surface area (m^2/g)	Bulk density (g/cm^3) Non impregnated	Average Dpore (Å)	LC (% (w/w))	Bulk density (g/cm^3) impregnated
C1(A)	469 (76)[a]	0.025 (0.003)[g]	202	60.5	0.093 (0.001)[e]
C2(A)	527 (31)[a]	0.026 (0.002)[g]	208	57.1	0.091 (0.002)[e]
C3(A)	525 (86)[a]	0.059 (0.004)[c]	137	57.6	0.285 (0.002)[b]
WRP (A)	524 (69)[a]	0.052 (0.002)[d]	137	59.3	0.304 (0.02)[a]
C1(B)	523 (53)[a]	0.035 (0.003)[f]	206	9.3	0.049 (0.004)[g]
C2(B)	537 (63)[a]	0.041 (0.003)[e]	207	19.4	0.070 (0.002)[f]
C3(B)	523 (57)[a]	0.104 (0.002)[a]	137	18.3	0.151 (0.005)[c]
WRP (B)	585 (62)[a]	0.070 (0.003)[b]	139	15.2	0.122 (0.003)[d]

The data are averages and standard deviations (brackets) of triplicate measurements. Values in each column with different superscript letters (a-d) indicates significant differences ($p < 0.05$) among samples.

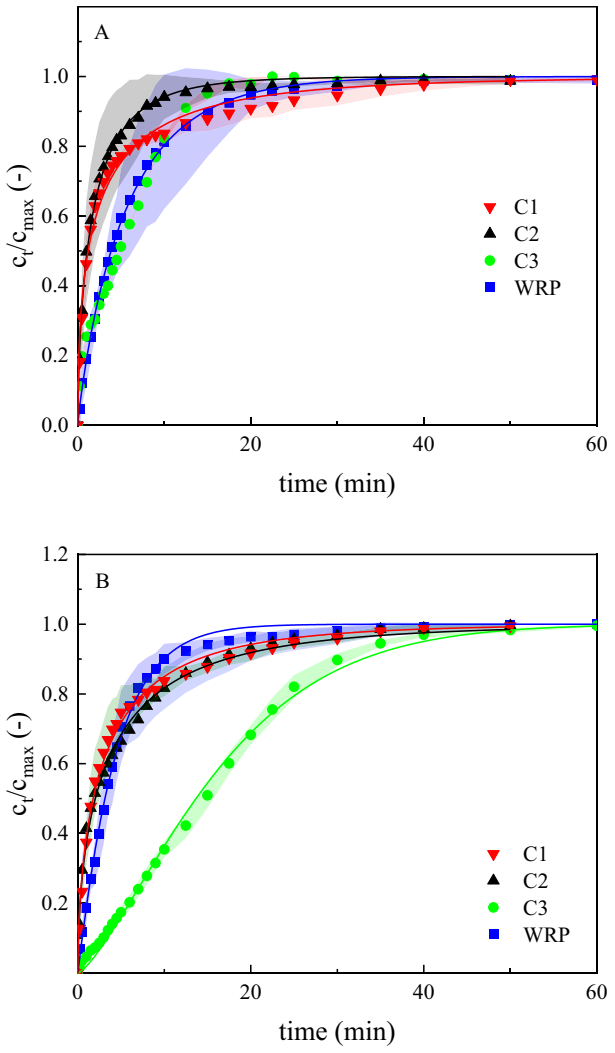

Fig. 5. Release patterns of vanillin from impregnated pectin beads (C1 (■), C2 (■), C3 (■) and WRP (■)) at (A) 2 and (B) 4 % (w/w). All data is averaged from 30, 40 and 50 °C release data and normalized to 100 % release. The solid lines correspond to Weibull model fitting. The shaded part of each line corresponds to standard deviation of the average of the three temperature values (30, 40 and 50 °C).

Table 4
Fitting of kinetic parameters and times of vanillin released to the media at 50 % (t50%) and 90 % (t90%) of the different impregnated pectin aerogels at (A) 2 % (w/w) and (B) 4 % (w/w).

Sample	R^2	α^{-1} (min^{-1})	β (−)	t50% (min)	t90% (min)
C1(A)	0.985	2.53(0.11)	0.49(0.02)	1.20	13.69
C2(A)	0.996	1.95(0.04)	0.63(0.01)	1.10	7.20
C3(A)	–	–	–	6.7[a]	12.4[a]
WRP(A)	0.999	5.81(0.04)	0.89(0.01)	3.96	14.77
C1(B)	0.991	3.35(0.10)	0.58(0.02)	1.80	13.96
C2(B)	0.994	3.9(0.10)	0.56(0.015)	2.05	17.26
C3(B)	0.997	17.9(0.24)	1.36(0.03)	13.69	32.91
WRP(B)	0.996	4.47(0.07)	1.04(0.02)	3.18	9.96

Mean value (standard deviation).
[a] Average point.

CRediT authorship contribution statement

D.A. Méndez: Methodology, Investigation, Formal analysis, Writing – original draft. **B. Schroeter:** Methodology, Investigation, Formal analysis. **A. Martínez-Abad:** Conceptualization, Writing – review & editing. **M.J. Fabra:** Conceptualization, Formal analysis, Supervision, Writing – review & editing. **P. Gurikov:** Conceptualization, Supervision, Writing – review & editing. **A. López-Rubio:** Conceptualization, Methodology, Funding acquisition, Project administration, Writing – review & editing.

Declaration of competing interest

The authors declare that they have no known competing financial interests or personal relationships that could have appeared to influence the work reported in this paper.

Data availability

Data will be made available on request.

Acknowledgments

D.A. Mendez is recipient of a predoctoral grant from the Ministry of Science Technology and Innovation of the Colombian Government (783-2017). D.A. Mendez also acknowledges financial support from the AERoGELS COST action CA18125 of the EU Horizon 2020 Framework Programme. The projects RTI2018-094268-B-C22 and CEX2021-001189-S were funded by MCIN/AEI/10.13039/501100011033 and by "ERDF A way of making Europe". Project INNEST/2021/27 was granted by Agencia Valenciana de Innovación (AVI) and co-financed by the European Union through the Operative Programme of FEDER from Comunitat Valenciana 2014–2020.

Appendix A. Supplementary data

Supplementary data to this article can be found online at https://doi.org/10.1016/j.carbpol.2023.120604.

References

Barrett, E. P., Joyner, L. G., & Halenda, P. P. (1951). The determination of pore volume and area distributions in porous substances. I. Computations from nitrogen isotherms. *Journal of the American Chemical Society, 73*(1), 373–380. https://doi.org/10.1021/ja01145a126

Benali, M., & Boumghar, Y. (2014). Supercritical fluid-assisted drying. In A. S. Mujumdar (Ed.), *Handbook of Industrial Drying* (pp. 1291–1300). CRC Press. https://doi.org/10.1201/b17208.

Bichara, L. C., Alvarez, P. E., Fiori Bimbi, M. V., Vaca, H., Gervasi, C., & Brandán, S. A. (2016). In , *76. Structural and spectroscopic study of a pectin isolated from citrus peel by using FTIR and FT-Raman spectra and DFT calculations* (pp. 315–327). https://www.sciencedirect.com/science/article/pii/S1350449516300688?via%3Dihub.

Brigand, G., Denis, A., Grall, M., & Lecacheux, D. (1990). Insight into the structure of pectin by high performance chromatographic methods. *Carbohydrate Polymers, 12*(1), 61–77. https://doi.org/10.1016/0144-8617(90)90104-Z

Brunauer, S., Emmett, P. H., & Teller, E. (1938). Adsorption of gases in multimolecular layers. *Journal of the American Chemical Society, 60*(2), 309–319. https://doi.org/10.1021/ja01269a023

Buchtová, N., & Budtova, T. (2016). Cellulose aero-, cryo- and xerogels: Towards understanding of morphology control. *Cellulose, 23*(4), 2585–2595. https://doi.org/10.1007/s10570-016-0960-8

Campbell, M., Lee, K. Y., Choo, W. S., Sandarani, M., Kute, A., Mohapatra, D., Babu, B., Sawant, B. P., Hartati, I., & Subekti, E. (2015). Extraction of pectin from watermelon rind. *Journal of Pharmacognosy & Natural Products, 03*(1), 1–8.

Chan, S. Y., Choo, W. S., Young, D. J., & Loh, X. J. (2017). Pectin as a rheology modifier: Origin, structure, commercial production and rheology. *Carbohydrate Polymers, 161*, 118–139. https://doi.org/10.1016/j.carbpol.2016.12.033

Chartier, C., Buwalda, S., Van Den Berghe, H., Nottelet, B., & Budtova, T. (2022). Tuning the properties of porous chitosan: Aerogels and cryogels. *International Journal of Biological Macromolecules, 202*, 215–223. https://doi.org/10.1016/j.ijbiomac.2022.01.042

Chen, H., Qiu, S., Gan, J., Liu, Y., Zhu, Q., & Yin, L. (2016). New insights into the functionality of protein to the emulsifying properties of sugar beet pectin. *Food Hydrocolloids, 57*, 262–270. https://doi.org/10.1016/j.foodhyd.2016.02.005

Dirauf, M. P., Hajnal, A., Gurikov, P., & Braeuer, A. S. (2021). Protein gel shrinkage during solvent exchange: Quantification of gel compaction, mass transfer and compressive strength. *Food Hydrocolloids, 120*, Article 106916. https://doi.org/10.1016/J.FOODHYD.2021.106916

Dronnet, V. M., Renard, C. M. G. C., Axelos, M. A. V., & Thibault, J. F. (1996). Characterisation and selectivity of divalent metal ions binding by citrus and sugar-beet pectins. *Carbohydrate Polymers, 30*(4), 253–263. https://doi.org/10.1016/S0144-8617(96)00107-5

el Fihry, N., el Mabrouk, K., Eeckhout, M., Schols, H. A., Filali-Zegzouti, Y., & Hajjaj, H. (2022). Physicochemical and functional characterization of pectin extracted from Moroccan citrus peels. *LWT- Food Science and Technology, 162*, Article 113508. https://doi.org/10.1016/J.LWT.2022.113508

El-naggar, M. E., Othman, S. I., Allam, A. A., & Morsy, O. M. (2020). Synthesis, drying process and medical application of polysaccharide-based aerogels. *International Journal of Biological Macromolecules, 145*, 1115–1128. https://doi.org/10.1016/j.ijbiomac.2019.10.037

Esparza, I., Jiménez-Moreno, N., Bimbela, F., Ancín-Azpilicueta, C., & Gandía, L. M. (2020). Fruit and vegetable waste management: Conventional and emerging approaches. *Journal of Environmental Management, 265*, Article 110510. https://doi.org/10.1016/j.jenvman.2020.110510

Fitri, A., Salahuddin, H., Izzuddin, M., Shafiq, I., Huda, Y., Radziah, R., & Hakimah, A. (2021). Optimisation of alginate-pectin bead formulation using central composite design guided electrospray technique. *International Food Research Journal, 28*(4), 860–870.

Frenkel, C., & Havna-Frenkel, D. (2006). Vanilla material properties: The physics and chemistry of vanillin - Research sheds light on practical ways to prevent losses of vanillin during production. *Perfumer and Flavorist, 31*(3).

García-González, C. A., Carenza, E., Zeng, M., Smirnova, I., & Roig, A. (2012). Design of biocompatible magnetic pectin aerogel monoliths and microspheres. *RSC Advances, 2*(26), 9816–9823. https://doi.org/10.1039/c2ra21500d

García-González, C. A., Jin, M., Gerth, J., Alvarez-Lorenzo, C., & Smirnova, I. (2015). Polysaccharide-based aerogel microspheres for oral drug delivery. *Carbohydrate Polymers, 117*, 797–806. https://doi.org/10.1016/j.carbpol.2014.10.045

García-González, C. A., Sosnik, A., Kalmár, J., de Marco, I., Erkey, C., Concheiro, A., & Alvarez-Lorenzo, C. (2021). Aerogels in drug delivery: From design to application. *Journal of Controlled Release, 332*, 40–63. https://doi.org/10.1016/J.JCONREL.2021.02.012

Gnanasambandam, R., & Proctor, A. (2000). Determination of pectin degree of esterification by diffuse reflectance Fourier transform infrared spectroscopy. *Food Chemistry, 68*(3), 327–332. https://doi.org/10.1016/S0308-8146(99)00191-0

Groult, S., & Budtova, T. (2018). Tuning structure and properties of pectin aerogels. *European Polymer Journal, 108*(July), 250–261. https://doi.org/10.1016/j.eurpolymj.2018.08.048

Groult, S., Buwalda, S., & Budtova, T. (2021a). Pectin hydrogels, aerogels, cryogels and xerogels: Influence of drying on structural and release properties. *European Polymer Journal, 149*, Article 110386. https://doi.org/10.1016/J.EURPOLYMJ.2021.110386

Groult, S., Buwalda, S., & Budtova, T. (2021b). Tuning bio-aerogel properties for controlling theophylline delivery. Part 1: Pectin aerogels. *Materials Science and EngineeringC, 126*, Article 112148. https://doi.org/10.1016/J.MSEC.2021.112148

Gurikov, P., SPR, Griffin, J. S., Steiner, S. A., & Smirnova, I. (2019). 110th anniversary: Solvent exchange in the processing of biopolymer aerogels: current status and open questions. *Industrial & Engineering Chemistry Research, 58*(40), 18590–18600. https://doi.org/10.1021/acs.iecr.9b02967

Hartati, I., & Subekti, E. (2015). Microwave assisted extraction of watermelon rind pectin. *International Journal of ChemTech Research, 8*(11), 163–170.

Kacuráková, M., Capek, P., Sasinková, V., Wellner, N., & Ebringerová, A. (2000). FT-IR study of plant cell wall model compounds: Pectic polysaccharides and hemicelluloses. *Carbohydrate Polymers, 43*(2), 195–203. https://doi.org/10.1016/S0144-8617(00)00151-X

Khedaioui, D., Boisson, C., D'Agosto, F., & Montarnal, D. (2019). Polyethylene aerogels with combined physical and chemical crosslinking: Improved mechanical resilience and shape-memory properties. *Angewandte Chemie International Edition, 58*(44), 15883–15889. https://doi.org/10.1002/ANIE.201908257

Kokkinidou, S., Floros, J. D., & Laborde, L. F. (2014). Kinetics of the thermal degradation of patulin in the presence of ascorbic acid. *Journal of Food Science, 79*(1), T108–T114. https://doi.org/10.1111/1750-3841.12316

Kozioł, A., Środa-Pomianek, K., Górniak, A., Wikiera, A., Cyprych, K., & Malik, M. (2022). Structural determination of pectins by spectroscopy methods. *Coatings, 12*(4). https://doi.org/10.3390/coatings12040546

Leven, F., Ulbricht, M., Limberg, J., & Ostermann, R. (2021). Novel finely structured polymer aerogels using organogelators as a structure-directing component. *Journal of Materials Chemistry A, 9*(36), 20695–20702. https://doi.org/10.1039/D1TA06161E

Liebner, F., Haimer, E., Potthast, A., Loidl, D., Tschegg, S., Neouze, M.-A., Wendland, M., & Rosenau, T. (2009). Cellulosic aerogels as ultra-lightweight materials. Part 2: Synthesis and properties 2nd ICC 2007, Tokyo, Japan, October 25–29, 2007. *Holzforschung, 63*(1), 3–11. https://doi.org/10.1515/HF.2009.002

Liu, J., Kim, Y., & McHugh, M. A. (2006). Phase behavior of the vanillin–CO2 system at high pressures. *The Journal of Supercritical Fluids, 39*(2), 201–205. https://doi.org/10.1016/J.SUPFLU.2006.01.006

Liu, Y., Wang, S., Li, J., Guo, S., Yan, H., Li, K., Tong, L., Gao, Y., Li, T., Chen, M., Gao, Z., & Gong, J. (2023). Preparation of ethyl vanillin spherical particles with functions of sustained release and anti-caking by an organic solvent-free process. *Food Chemistry, 402*, Article 134518. https://doi.org/10.1016/J.FOODCHEM.2022.134518

Manzocco, L., Mikkonen, K. S., & García-González, C. A. (2021). Aerogels as porous structures for food applications: Smart ingredients and novel packaging materials. *Food Structure, 28*, Article 100188. https://doi.org/10.1016/j.foostr.2021.100188

Mehling, T., Smirnova, I., Guenther, U., & Neubert, R. H. H. (2009). Polysaccharide-based aerogels as drug carriers. *Journal of Non-Crystalline Solids, 355*(50–51), 2472–2479. https://doi.org/10.1016/j.jnoncrysol.2009.08.038

Méndez, D. A., Fabra, M. J., Gómez-Mascaraque, L., López-Rubio, A., & Martinez-Abad, A. (2021). Modelling the extraction of pectin towards the valorisation of watermelon rind waste. *Foods, 10*(4), 738. https://doi.org/10.3390/foods10040738

Mendez, D. A., Fabra, M. J., Martínez-Abad, A., Martínez-Sanz, M., Gorria, M., & López-Rubio, A. (2021). Understanding the different emulsification mechanisms of pectin: Comparison between watermelon rind and two commercial pectin sources. *Food Hydrocolloids, 120*, Article 106957. https://doi.org/10.1016/j.foodhyd.2021.106957

Méndez, D. A., Martínez-Abad, A., Martínez-Sanz, M., López-Rubio, A., & Fabra, M. J. (2022). Tailoring structural, rheological and gelling properties of watermelon rind pectin by enzymatic treatments. *Food Hydrocolloids, 108119*. https://doi.org/10.1016/j.foodhyd.2022.108119

Mikshina, P. V., Makshakova, O. N., Petrova, A. A., Gaifullina, I. Z., Idiyatullin, B. Z., Gorshkova, T. A., & Zuev, Y. F. (2017). Gelation of rhamnogalacturonan I is based on galactan side chain interaction and does not involve chemical modifications. *Carbohydrate Polymers, 171*, 143–151. https://doi.org/10.1016/j.carbpol.2017.05.013

Ne, A., Gordi, M., Davidovi, S., Radovanovi, Ž., Nedeljkovi, J., Smirnova, I., Gurikov, P., Nešić, A., Gordić, M., Davidović, S., Radovanović, Ž., Nedeljković, J., Smirnova, I., & Gurikov, P. (2018). Pectin-based nanocomposite aerogels for potential insulated food packaging application. *Carbohydrate Polymers, 195*(March), 128–135. https://doi.org/10.1016/j.carbpol.2018.04.076

Ngouémazong, D. E., Jolie, R. P., Cardinaels, R., Fraeye, I., van Loey, A., Moldenaers, P., & Hendrickx, M. (2012). Stiffness of ca 2+-pectin gels: Combined effects of degree and pattern of methylesterification for various ca 2+ concentrations. *Carbohydrate Research, 348*, 69–76. https://doi.org/10.1016/j.carres.2011.11.011

Ngouémazong, D. E., Kabuye, G., Fraeye, I., Cardinaels, R., van Loey, A., Moldenaers, P., & Hendrickx, M. (2012). Effect of debranching on the rheological properties of Ca2+-pectin gels. *Food Hydrocolloids, 26*(1), 44–53. https://doi.org/10.1016/j.foodhyd.2011.04.009

Pasandide, B., Khodaiyan, F., Mousavi, Z. E., & Hosseini, S. S. (2017). Optimization of aqueous pectin extraction from Citrus medica peel. *Carbohydrate Polymers, 178*, 27–33. https://doi.org/10.1016/j.carbpol.2017.08.098

Petkowicz, C. L. O., Vriesmann, L. C., & Williams, P. A. (2017). Pectins from food waste: Extraction, characterization and properties of watermelon rind pectin. *Food Hydrocolloids, 65*, 57–67. https://doi.org/10.1016/j.foodhyd.2016.10.040

Preibisch, I., Niemeyer, P., Yusufoglu, Y., Gurikov, P., Milow, B., & Smirnova, I. (2018). Polysaccharide-based aerogel bead production via jet cutting method. *Materials, 11*(8). https://doi.org/10.3390/ma11081287

Rodríguez-Dorado, R., López-Iglesias, C., García-González, C. A., Auriemma, G., Aquino, R. P., & Del Gaudio, P. (2019). Design of aerogels, cryogels and xerogels of alginate: Effect of molecular weight, gelation conditions and drying method on particles' micromeritics. *Molecules, 24*(6). https://doi.org/10.3390/molecules24061049

Rojas-Ávila, A., Pimentel-Rodas, A., Rosales-García, T., Dávila-Ortiz, G., & Galicia-Luna, L. A. (2016). Solubility of binary and ternary systems containing vanillin and vanillic acid in supercritical carbon dioxide. *Journal of Chemical and Engineering Data, 61*(9), 3225–3232. https://doi.org/10.1021/ACS.JCED.6B00322/ASSET/IMAGES/JE-2016-00322X_M005.GIF

Rupasinghe, H. P. V., Boulter-Bitzer, J., Ahn, T., & Odumeru, J. A. (2006). Vanillin inhibits pathogenic and spoilage microorganisms in vitro and aerobic microbial growth in fresh-cut apples. *Food Research International, 39*(5), 575–580. https://doi.org/10.1016/J.FOODRES.2005.11.005

Schroeter, B., Bettermann, S., Semken, H., Melchin, T., Weitzel, H. P., & Pauer, W. (2019). Kinetic description of ascorbic acid decomposition in redox initiator systems for polymerization processes. *Industrial and Engineering Chemistry Research, 58*(29), 12939–12952. https://doi.org/10.1021/ACS.IECR.9B00710/ASSET/IMAGES/MEDIUM/IE-2019-007109_M013.GIF

Schroeter, B., Yonkova, V. P., Goslinska, M., Orth, M., Pietsch, S., Gurikov, P., Smirnova, I., & Heinrich, S. (2021a). Spray coating of cellulose aerogel particles in a miniaturized spouted bed. *Cellulose, 28*(12), 7795–7812. https://doi.org/10.1007/s10570-021-04032-0

Schroeter, B., Yonkova, V. P., Niemeyer, N. A. M. M., Jung, I., Preibisch, I., Gurikov, P., & Smirnova, I. (2021). Cellulose aerogel particles: Control of particle and textural properties in jet cutting process. *Cellulose, 28*(1), 223–239. https://doi.org/10.1007/s10570-020-03555-2

Shi, P., He, P., Teh, T. K. H., Morsi, Y. S., & Goh, J. C. H. (2011). Parametric analysis of shape changes of alginate beads. *Powder Technology, 210*(1), 60–66. https://doi.org/10.1016/J.POWTEC.2011.02.023

Siepmann, J., & Siepmann, F. (2012). Modeling of diffusion controlled drug delivery. *Journal of Controlled Release, 161*(2), 351–362. https://doi.org/10.1016/J.JCONREL.2011.10.006

Sinha, A. K., Sharma, U. K., & Sharma, N. (2009). A comprehensive review on vanilla flavor: Extraction, isolation and quantification of vanillin and others constituents. *59*(4), 299–326. https://doi.org/10.1080/09687630701539350

Stanzione, M., Gargiulo, N., Caputo, D., Liguori, B., Cerruti, P., Amendola, E., Lavorgna, M., & Buonocore, G. G. (2017). Peculiarities of vanillin release from amino-functionalized mesoporous silica embedded into biodegradable composites. *European Polymer Journal, 89*, 88–100. https://doi.org/10.1016/J.EURPOLYMJ.2017.01.040

Sun, R., & Hughes, S. (1998). Extraction and physico-chemical characterization of pectins from sugar beet pulp. *Polymer Journal, 30*(8), 671–677. https://doi.org/10.1295/polymj.30.671

Thibault, J. F., & Rinaudo, M. (1986). Chain association of pectic molecules during calcium-induced gelation. *Biopolymers, 25*(3), 455–468. https://doi.org/10.1002/BIP.360250306

Tkalec, G., Knez, Ž., & Novak, Z. (2016). PH sensitive mesoporous materials for immediate or controlled release of NSAID. *Microporous and Mesoporous Materials, 224*, 190–200. https://doi.org/10.1016/J.MICROMESO.2015.11.048

Tromelin, A., Andriot, I., & Guichard, E. (2006). Protein–flavour interactions. In *Flavour in Food* (pp. 172–207). Elsevier. https://doi.org/10.1533/9781845691400.2.172.

Veronovski, A., Tkalec, G., Knez, Z., & Novak, Z. (2014a). Characterisation of biodegradable pectin aerogels and their potential use as drug carriers. *Carbohydrate Polymers, 113*, 272–278. https://doi.org/10.1016/J.CARBPOL.2014.06.054

White, R. J., Budarin, V. L., & Clark, J. H. (2010). Pectin-derived porous materials. *Chemistry - A European Journal, 16*(4), 1326–1335. https://doi.org/10.1002/CHEM.200901879

Zubairu, A., Gimba, A. S. B., Mamza, W. J., & Highina, B. K. (2018). Proximate analysis of dry watermelon (Citrullus lanatus) rind and seed powder. Available Online Www.Jsaer.Com *Journal of Scientific and Engineering Research, 5*(3), 473–478.